

## Microbending Loss and Stresses Induced by both Temperature Variation and Axial Strain in Multi-coated Optical Fibers

Moustafa H. Aly\*, A. M. Shoaeb, M. S. Helmi, M. Reyad

### Summary

The microbending loss and the stresses induced by both the temperature variation and the axial strain in multi-coated optical fibers are studied. Optical fibers with two up to six coatings are considered. A recurrence relation is obtained for the lateral pressure on the glass fiber, from which the microbending loss and the stresses are calculated. It is found that the microbending loss can be minimized by increasing the number of coatings.

### 1 Introduction

Optical fiber cables must be designed so that transmission characteristics of the fiber are maintained after the cabling process and cable installation. Certain problems may occur either within the cabling process or subsequently which can significantly affect the fiber transmission characteristics. The most important one is the meandering of the fiber axis on a microscopic scale with the cable form. This phenomenon, known as microbending, results from small lateral forces exerting on the fiber. These lateral forces are caused externally by axial stresses and internally by thermal ones. This yields losses due to radiation in both multimode and single-mode fibers.

Mechanical and thermal stresses play an important role in optical fibers, so, they have been studied extensively. Several reports have appeared on the temperature characteristics of jacketed optical fibers. D. Glöge computed the excess transmission loss resulting from statistical surface variations and lateral pressures affecting the fiber [1]. The loss induced in optical fibers by random bends in the fiber axis was studied experimentally by winding fibers under constant tension on to a drum surface that is not perfectly smooth [2]. The shrinkage of a plastic jacket at low temperature causes microbends in the optical fibers and consequently an excess loss which increases suddenly at low temperature due to the fiber buckling [3]. The thermal stresses and the added transmission loss in both single and double-coated optical fibers at low temperature were calculated by Suhir [4] and Shiu [5]. Shiu evaluated the microbending loss induced by axial strain in double-coated optical fibers as well as the thermal stresses in tightly jacketed double-coated optical fibers at low temperature [6, 7].

However, to the best of our knowledge, no work has been done on the problem of microbending loss induced by both external axial strain and thermal stresses in multi-coated optical fibers at low temperature. In this study we derived a recurrence relation for the lateral pressure and, consequently, the microbending loss in a multi-coated optical fibers. The objective of this study is to determine the best number of coatings which gives minimum added microbending loss. This can be accomplished by noting that the lateral pressure should be tensile, i. e., it should have a negative value. As a result, the optical properties of the fiber will not be affected under this condition [6].

### 2 Analysis

#### 2.1 Lateral pressures

##### 2.1.1 Thermal stresses

Figure 1 illustrates the fiber under consideration which is constructed of a glass (core and cladding) coated by  $n$  polymeric layers. The radii of glass fiber cladding, primary coating, and  $n$ th coating are  $r_0$ ,  $r_1$ , and  $r_n$ , respectively.

The optical fiber is assumed infinite along the axial direction. Because the physical properties (e.g. Young's modulus and coefficient of thermal expansion) of the glass and polymeric coatings are different and assuming zero stress in the system at the initial temperature, stress will be built up after the temperature drop. Assuming the glass fiber is rigid compared with the polymeric coatings and the viscoelastic behavior of polymeric coating is not considered, then the thermal stresses in the multi-coated optical fiber can be solved starting from the Lamé formulae as follows [8]:

---

#### Address of authors:

\* Engineering Mathematics and Physics Department  
Faculty of Engineering, University of Alexandria  
Alexandria 21544, Egypt

Physics Department, Faculty of Science  
University of Alexandria

Received 11 October 1996

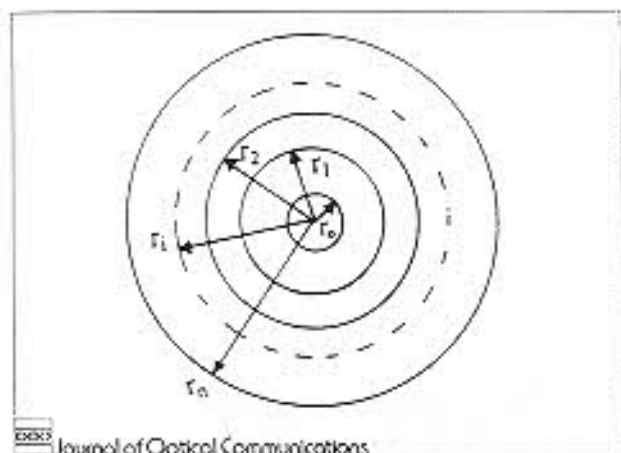


Fig. 1: Schematic diagram of a multicoated optical fiber

The Lamé formulae for the radial stress  $\sigma_r$ , and the tangential stress  $\sigma_\theta$ , in a circular thick-walled tube subjected to internal pressure  $p_i$  and external pressure  $p_e$  are [8]:

$$\sigma_r = \frac{a^2 b^2 (p_e - p_i)}{r^2 (b^2 - a^2)} + \frac{a^2 p_i - b^2 p_e}{b^2 - a^2} \quad (1a)$$

and

$$\sigma_\theta = -\frac{a^2 b^2 (p_e - p_i)}{r^2 (b^2 - a^2)} + \frac{a^2 p_i - b^2 p_e}{b^2 - a^2} \quad (1b)$$

where  $a$  and  $b$  are the inner and outer radii of the tube, respectively. The radial ( $\epsilon_r$ ), tangential ( $\epsilon_\theta$ ) and axial ( $\epsilon_z$ ) strains are given by [8]

$$\epsilon_r = -\alpha \Delta T + \frac{1}{E} [\sigma_r - \nu (\sigma_\theta + \sigma_z)] \quad (2a)$$

$$\epsilon_\theta = -\alpha \Delta T + \frac{1}{E} [\sigma_\theta - \nu (\sigma_z + \sigma_r)] \quad (2b)$$

and

$$\epsilon_z = -\alpha \Delta T + \frac{1}{E} [\sigma_z - \nu (\sigma_r + \sigma_\theta)] \quad (2c)$$

where  $E$ ,  $\alpha$ , and  $\nu$  are the Young's modulus, coefficient of thermal expansion, and Poisson's ratio of the material, respectively. Here, the temperature drop  $\Delta T$  is larger than zero. Because the fiber is assumed infinite and both ends are fastened, the plane strain is adopted, i. e. the axial strain  $\epsilon_z$  is zero. Due to geometric symmetry, only the radial displacement  $u$  is not zero.

The radial and tangential strains are related to the radial displacement  $u$  by the following equations [8]

$$\epsilon_\theta = \frac{u}{r} \quad (3)$$

Using (1), (2) and (3), the radial displacement,  $u$ , is obtained as:

$$u = -\alpha \Delta T (1 + \nu) r + \frac{1 + \nu}{E(1 - \gamma^2)} \left[ r(1 - 2\nu) (p_i \gamma^2 - p_e) - \frac{a^2}{r} (p_e - p_i) \right] \quad (4)$$

where  $\gamma = a/b$ .

(4) is used to evaluate the thermal radial displacement at each boundary starting from the cladding and first coating interface. We've obtained general forms for the thermal displacements,  $u_{i-1,i}$  and  $u_{ii}$ , for both of the outer boundary of the coating  $i-1$  and the inner boundary of the coating  $i$  as

$$u_{i-1,i} = -\alpha_{i-1} r_{i-1} \Delta T (1 + \nu_{i-1}) + \frac{r_{i-1} (1 + \nu_{i-1})}{E_{i-1} (1 - \gamma_{i-1}^2)} \left[ 2p_{i-1} \gamma_{i-1}^2 (1 - \nu_{i-1}) - p_i (1 - 2\nu_{i-1} + \gamma_{i-1}^2) \right] \quad (5a)$$

and

$$u_{ii} = -\alpha_i \Delta T (1 + \nu_i) r_{i-1} + \frac{r_{i-1} (1 + \nu_i)}{E_i (1 - \gamma_{i-1}^2)} \left[ p_i + p_i \gamma_i^2 (1 + 2\nu_i) - 2(1 - \nu_i) p_{i+1} \right] \quad (5b)$$

where  $i = 1, 2, \dots, n$ . The conditions for compatibility of displacements are [8]:

$$u_{i-1,i} = u_{ii} \quad (6)$$

Using (6) and after algebraic manipulation, one can get a recurrence relation for the lateral pressures as:

$$R_{n-j} p_{n-j} = Q_{n-j} + T_{n-j} p_{n-j-1} \quad (7)$$

where  $j = 0, 1, \dots, n-1$  and the coefficients  $R_{n-j}$ ,  $Q_{n-j}$ ,  $T_{n-j}$  are functions of the fiber and coatings parameters. (7) can be used to calculate the lateral pressure on the fiber glass for any number of coatings.

### 2.1.2 Axial strain

In this case, the optical fiber is subjected to an external axial strain  $\epsilon_z$ . The stress-strain relations are obtained by putting  $\Delta T = 0$  in (2). Eliminating  $\sigma_z$  from these relations, one can get the tangential and radial strains as:

$$\epsilon_\theta = -\nu \epsilon_z + \frac{1 - \nu^2}{E} \left( \sigma_\theta - \frac{\nu \sigma_r}{1 - \nu} \right) \quad (8a)$$

and

$$\epsilon_r = -\nu \epsilon_z + \frac{1 - \nu^2}{E} \left( \sigma_r - \frac{\nu \sigma_\theta}{1 - \nu} \right) \quad (8b)$$

In a similar manner to the thermal stress analysis, (3) and (8a) can be used to get the radial displacement  $u$ , as:

$$u = -\nu \epsilon_z r + \frac{r(1 - \nu^2)}{E} \left( \sigma_\theta - \frac{\nu \sigma_r}{1 - \nu} \right) \quad (9)$$

By comparison, (7) can be used in the calculation of the lateral pressures, however the coefficient  $Q_{j-1}$  will be changed.

### 2.1.3 The general case

Here the optical fiber will be subject to both external axial strain and temperature variations. The total axial stress is given directly from (2c) as

$$\sigma_z = \epsilon_z E + \alpha \Delta T E + \nu(\sigma_r + \sigma_\theta). \quad (10)$$

Following the same procedure previously described, one gets the total radial displacement as:

$$u = -\alpha \Delta T r(1 + \nu) - \nu \epsilon_z r + \frac{r(1 - \nu^2)}{E} \left[ \sigma_\theta - \frac{\nu \sigma_r}{1 - \nu} \right] \quad (11)$$

Again, changing the coefficient  $Q_{j-1}$ , then (7) is practicable. Hence, using this equation, the lateral pressures can be evaluated as a function of the physical properties of the optical fiber as well as the environmental conditions.

## 2.2 Microbending loss

The compressive lateral pressure,  $p_i$ , in the glass fiber would produce excess microbending loss, so it should be minimized [4]. For  $j = n-1$  in (7) the lateral pressure,  $p_i$ , can be written in the form

$$p_i = \frac{Q_i}{R_i}. \quad (12)$$

The microbending loss,  $\alpha$ , can be evaluated from the lateral pressure,  $p_i$ , through the linear relation [6]

$$\alpha = G p_i, \quad (13)$$

where  $G$  is a constant, which has the experimentally determined value of 0.0029 (dB/km)/MPa [5].

Obviously, the developed recurrence relations can be used to calculate the lateral pressure and consequently the microbending loss induced in multi-coated optical fibers.

## 2.3 Normal stresses

Based on (1) and putting  $a = 0$ ,  $p_i = 0$  and  $p_e = p_i$ , the radial stress  $\sigma_r$  and the tangential stress  $\sigma_\theta$  in the glass fiber will simply equal to  $-p_i$ . However, the corresponding stresses in the  $i$ th coating will have forms:

$$\sigma_r = \frac{r_{i-1}^2 - r_i^2 (p_{i+1} - p_i)}{r^2 (r_i^2 - r_{i-1}^2)} + \frac{p_i r_{i-1}^2 - p_{i+1} r_i^2}{r_i^2 - r_{i-1}^2}, \quad (14a)$$

and

$$\sigma_\theta = -\frac{r_{i-1}^2 - r_i^2 (p_{i+1} - p_i)}{r^2 (r_i^2 - r_{i-1}^2)} + \frac{p_i r_{i-1}^2 - p_{i+1} r_i^2}{r_i^2 - r_{i-1}^2}, \quad (14b)$$

where  $r_{i-1} \leq r \leq r_i$ .

In the case of axial stress,  $\sigma_z$ , it is desirable to discuss the general case, where thermal stresses are included. According to (2),  $\sigma_z$  in the glass fiber and in the  $i$ th coating are given respectively by:

$$\sigma_z = E_0 \alpha_0 \Delta T + E_0 \epsilon_z - 2\nu_0 p_i, \quad 0 \leq r \leq r_0 \quad (15)$$

and

$$\sigma_z = 2\nu_i \frac{p_i r_{i-1}^2 - p_{i+1} r_i^2}{r_i^2 - r_{i-1}^2} + E_i (\epsilon_z + \alpha_i \Delta T), \quad r_{i-1} \leq r \leq r_i \quad (16)$$

It is clear that  $\sigma_z$  is uniform within each medium. However, both  $\sigma_r$  and  $\sigma_\theta$  are dependent on  $r$  except for the region  $0 \leq r \leq r_0$ , (14). Thus, the tangential and the radial stresses are uniform in the glass fiber. This will not be the case if any lateral pressure on the core-cladding interface is considered. For instance, if  $p_0$  is not equal zero, then  $p_i$  will be given by:

$$p_i = \frac{Q_i}{R_i} + \frac{p_0 T_i}{R_i}, \quad (17)$$

and  $p_0$  will be calculated from (7) by allowing the value  $n$  for  $j$ . Hence, the Young's modulus, the coefficient of thermal expansion, and Poisson's ratio must be considered separately for both the core and cladding in any calculations. In addition,  $\sigma_r$  and  $\sigma_\theta$  are independent on  $r$  in the core only.

(14a) indicates that as  $r$  increases, the radial stress changes from the initial value  $-p_i$  till the final value  $p_{i+1}$  which is assumed to be zero. However, the sign of the lateral pressure depends on the values of  $E$ ,  $\nu$ , and  $\gamma$ . Therefore, the radial stress may increase or decrease as  $1/r^2$  depending on the sign of the lateral pressures. On the other hand, the dependence of  $\sigma_\theta$  on  $r$  is the opposite, because of the negative sign in (14b).

## 3 Results and discussion

A computer program is developed for the purpose of lateral pressure calculations in optical fibers. For evaluation purposes, this program has been used to calculate the lateral pressure  $p_i$  using the parameters in the first and second designs of Shiue [5, 6]. The results are identical to that obtained in both cases; namely the axial strain and temperature variation. Furthermore, the lateral pressure relations derived by Shiue are obtained analytically [5, 6]. This gives us the confidence regarding the wider use of the model in the case of multi-coated optical fibers.

The value of  $p_i$  depends on the elastic properties of both the optical fiber and the coatings as well as their radii. In addition, for a real polymeric coating material the Young's modulus,  $E$ , and the coefficient of thermal expansion,  $\alpha$ , are dependent on each other and could be characterized by a linear relationship [4]

$$\alpha = \alpha_* \left( 1 - \frac{E}{E_*} \right), \quad (18)$$

where  $\alpha_*$  is the coefficient of thermal expansion for a polymeric material with a very low Young's modulus, and  $E_*$  is the Young's modulus for a polymeric material

with a very low coefficient of thermal expansion. The values of  $\alpha_0$  and  $E_0$  are  $6.89 \cdot 10^{-5} \text{ K}^{-1}$  and  $11.35 \text{ GPa}$ , respectively [4]. We have considered the general case in which the optical fiber is subjected to a temperature drop  $\Delta T = 100 \text{ K}$  as well as an axial strain  $\epsilon_z = 0.001$  [9]. Furthermore, the parameters of the optical fibers under consideration are shown in Table 1. For  $n = 2$  (double coated optical fiber), these parameters are those considered by Shiue [6]. In addition, the optical fiber is assumed to be rigid so that  $E_0 \gg E_1$  and  $\alpha_0 \ll \alpha_1$ , and the cladding radius  $r_0 = 62.5 \mu\text{m}$ .

Table 1: The parameters of the optical fibers under consideration

n	$\nu$	E (MPa)	r ( $\mu\text{m}$ )
1	0.35	10	100
2	0.35	1200	125
3	0.35	2755	200
4	0.35	3600	250
5	0.35	4290	400
6	0.35	5790	500

Based on (18), the effects of thicknesses of the primary and the secondary coatings on the lateral pressure in the glass fiber are shown in Figs. 2 and 3, respectively.

It can be seen from Fig. 2 that  $p_1$  decreases with the thickness of the primary coating to very small positive values except for the fiber with  $n = 6$ . In this case,  $p_1$  becomes negative for  $r_1/r_0 > 1.62$ , and consequently there is no added microbending loss. Therefore, it is recommended that the thickness of the primary coating should be increased. It may be also noted from Fig. 3 that  $p_1$  takes small negative values at  $n = 6$  provided that  $r_2/r_1 > 1.26$ . Obviously, as the number of coating increases the curve of  $p_1$  vs  $r_2/r_1$  approaches zero.

The influence of Poisson's ratio of the primary coating on the lateral pressure is illustrated in Fig. 4. For  $n = 5$  and  $n = 6$ ,  $p_1$  takes the closest values to the zero, and it turns negative at  $\nu_1 \approx 0.45$  and  $0.36$ , respectively. However, as  $\nu_1$  increases the lateral pressure, in the former case ( $n = 5$ ), takes higher negative values faster than the later ( $n = 6$ ). Therefore, the fiber with  $n = 6$  is more practicable since it maintains the smallest negative values for  $p_1$  when  $\nu_1$  changes appreciably. It can be observed from Fig. 5 that  $p_1$  is negative for  $n = 6$  only at  $\nu_2 > 0.36$ . Figure 6 shows the relation between  $p_1$  and  $E_1$ . Generally,  $p_1$  increases with  $E_1$  and takes higher positive values, so, there is a microbending loss in this case. Obviously, the Young's modulus of the primary coating must be assigned small values to minimize  $p_1$ . However, as Fig. 7 indicates that  $E_2$  yields values of  $p_1$  larger than  $-0.05 \text{ MPa}$  for  $n = 6$  only. It can be noted that  $p_1$  becomes compressive if  $E_2 > 1200 \text{ MPa}$  approximately.

The effect of the physical properties of the higher coatings on  $p_1$  is also studied. It is found that the dependence of  $p_1$  on these parameters is the same as that obtained for the first and the second coatings. So, it is clear that as  $n$  increases the lateral pressure on the optical fiber decreases. In addition, the lateral pressure can be kept tensile with negligible values by choosing the suitable

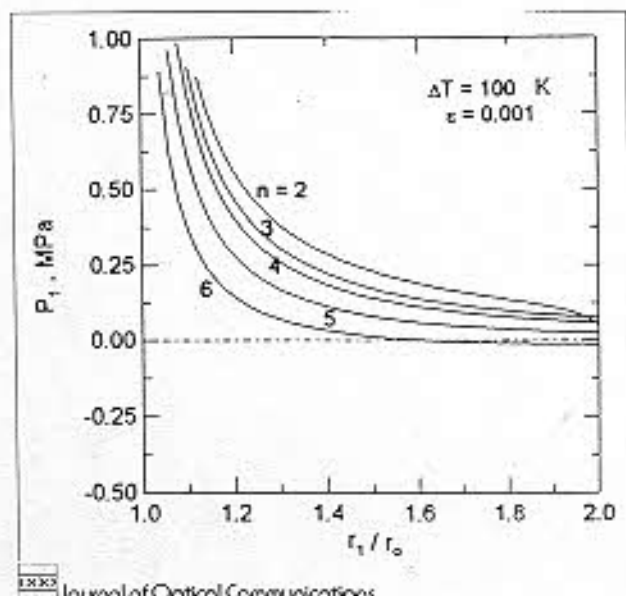


Fig. 2: Effect of thickness of primary coating  $r_1/r_0$  on the lateral pressure,  $p_1$ , in the glass fiber

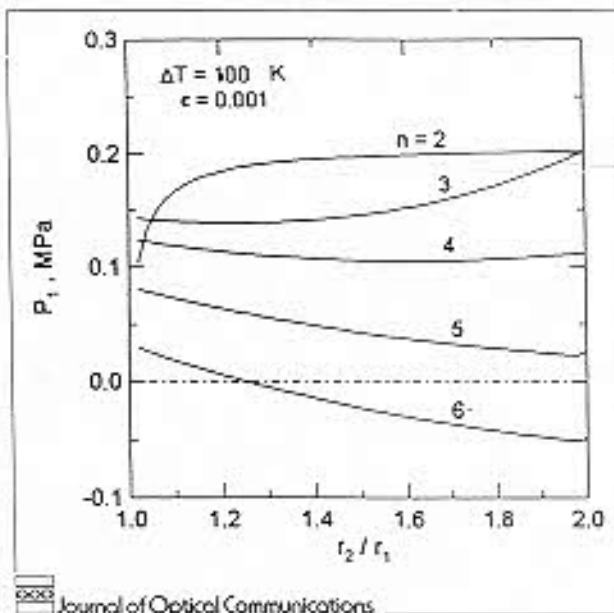


Fig. 3: Effect of thickness of secondary coating  $r_2/r_1$  on the lateral pressure,  $p_1$ , in the glass fiber

coating materials. On the other hand,  $p_1$  should be assigned a suitable negative value to avoid any transition to the compressive region.

#### 4 Conclusions

The microbending and the stresses induced by both the temperature variation and the external axial strain in multi-coated optical fibers are studied. The microbending due to the temperature variation is additive to that induced by the axial strain. Both the microbending losses and the stresses are proportional to the temperature variation and to the axial strain. In addition, they depend on the physical properties of the coating materials as well as their radii. In order to maintain the optical fiber

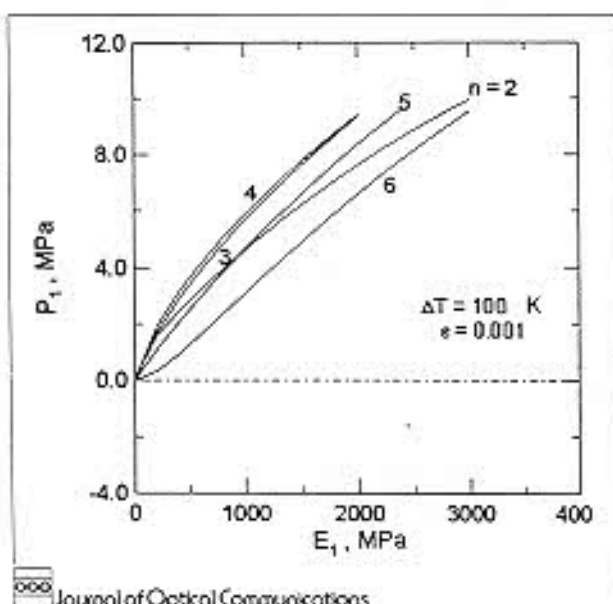


Fig. 4: Effect of Young's modulus of primary coating  $E_1$  on the lateral pressure,  $p_1$ , in the glass fiber

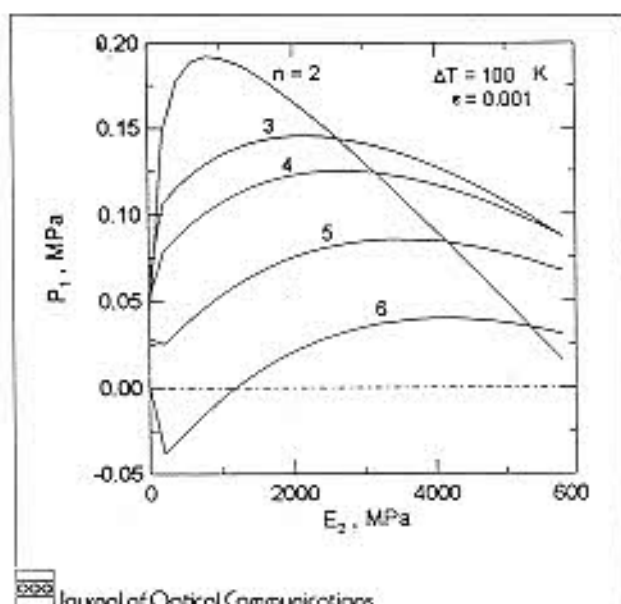


Fig. 5: Effect of Young's modulus of secondary coating  $E_2$  on the lateral pressure,  $p_1$ , in the glass fiber

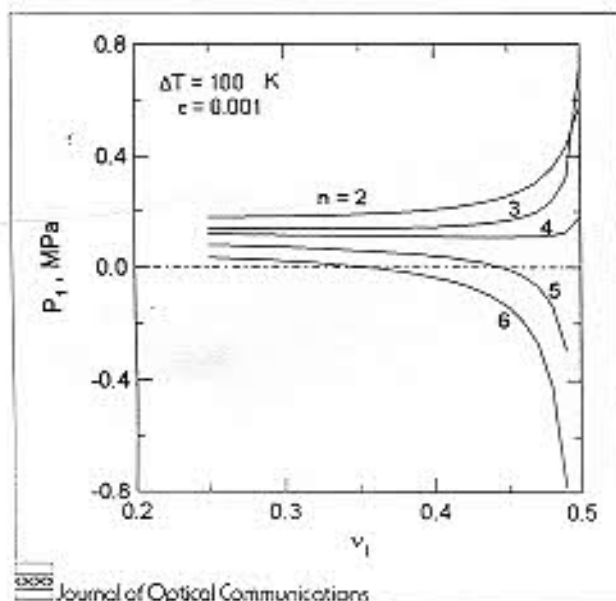


Fig. 6: Effect of Poisson's ratio of primary coating  $\nu_1$  on the lateral pressure,  $p_1$ , in the glass fiber

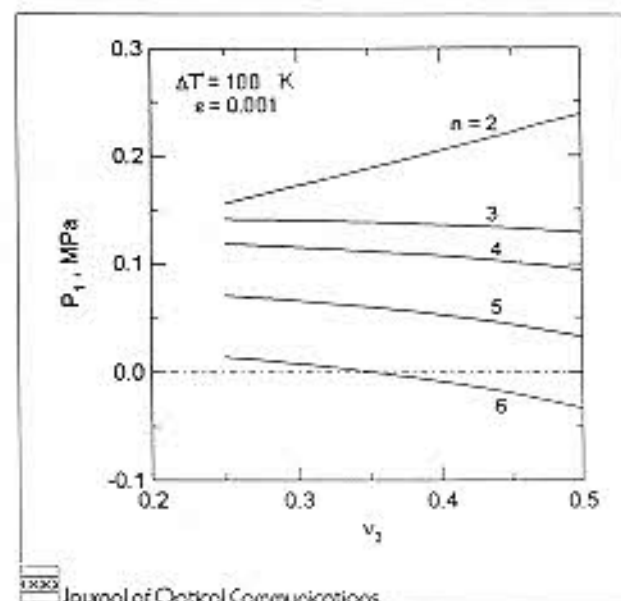


Fig. 7: Effect of Poisson's ratio of secondary coating  $\nu_2$  on the lateral pressure,  $p_1$ , in the glass fiber

without excess microbending loss the lateral pressure  $p_1$  must be tensile. The conditions under which  $p_1$  is tensile are determined for the optical fiber with  $n = 6$ . It is found that the lateral pressure  $p_1$ , and hence the microbending loss, on the glass fiber can be minimized by increasing the number of coatings. The final selection of the most suitable coating design must be based on the material, the optical, the chemical, and the cost consideration.

## References

- [1] D. Gloge: "Optical-Fiber Packaging and Its Influence on Fiber Straightness and Loss"; *Bell Syst. Tech. J.* 54 (1975) 2, 245-262
- [2] W. B. Gardner: "Microbending loss in optical fibers"; *Bell Syst. Tech. J.* 54 (1975) 2, 457-465
- [3] T. Yabuta, N. Yoshizawa, K. Ishihara: "Excess loss of single-mode jacketed optical fiber at low temperature"; *Appl. Opt.* 22 (1983) 15, 2356-2362
- [4] E. Suhic: "Mechanical Approach to the Evaluation of the Low Temperature Threshold of Added Transmission Losses in Single-Coated Optical Fibers"; *IEEE J. Lightwave Technol.* 8 (1990) 6, 863-868
- [5] S. T. Shiue, S.-J. Lee: "Thermal stresses in double-coated optical fibers at low temperature"; *J. App. Phys.* 72 (1992) 18, 18-23
- [6] S. T. Shiue: "Axial strain-induced microbending losses in double-coated optical fibers"; *J. App. Phys.* 73 (1993) 15, 526-529
- [7] S. T. Shiue: "Thermal stresses in tightly jacketed double-coated optical fibers at low temperature"; *J. App. Phys.* 76 (1994) 15, 7695-7705
- [8] S. Timoshenko, J.N. Goodier: "Theory of Elasticity", 2nd ed., McGraw-Hill Book Company, Inc., 1951
- [9] Morton I. Schwartz, Paul F. Gagen, Manuel R. Santana: "Fiber Cable Design and Characterization"; *Proc. IEEE* 68 (1980) 10, 1214-1219